Randomly charged polymers: An exact enumeration study

Yacov Kantor
School of Physics and Astronomy, Tel Aviv University, Tel Aviv 69 978, Israel

Mehran Kardar
Department of Physics, Massachusetts Institute of Technology, Cambridge, Massachusetts 02139
(Received 27 February 1995)

We perform an exact enumeration study of polymers formed from a (quenched) random sequence of charged monomers $\pm q_0$. Such polymers, known as polyampholytes, are compact when completely neutral and expanded when highly charged. Our exhaustive search includes all spatial conformations and quenched sequences for up to 12-step (13-site) walks. We investigate the behavior of the polymer as a function of its overall excess charge Q and temperature T. At low temperatures there is a phase transition from compact to extended configurations when the charge exceeds $Q_c \approx q_0\sqrt{N}$. There are also indications of a transition for small Q between two compact states on varying temperature. Numerical estimates are provided for the condensation energy, surface tension, and the critical exponent ν.

PACS number(s): 36.20.−r, 33.15.−e, 64.60.−i, 41.20.−q

I. INTRODUCTION

Given their ubiquity in nature, long chain macromolecules have been the subject of considerable study. Whereas there is now a reasonably firm basis for understanding the physical properties of homopolymers [1], considerably less is known about the heteropolymers of biological significance. From a biologist's perspective, it is the specific properties of a particular molecule that are of interest. After all, the genetic information is coded by very specific sequences of nucleic acids, which are in turn translated to the chain of amino acids forming a protein [2]. The energy of the polymer is determined by the van der Waals, hydrogen bonding, hydrophobic or hydrophilic, and Coulomb interactions between its constituent amino acids. In accord to these interactions, the protein folds into a specific shape that is responsible for its activity. Given the large number of monomers making up such chains, and the complexity of their interactions, finding the configuration of a particular molecule is a formidable task. In contrast, a physicist's approach is to sacrifice the specificity, in the hope of gleaning some more general information from simplified models [3]. There are, in fact, a number of statistical descriptions of *ensembles* of molecules composed of a random linear sequence of elements with a variety of interactions that determine their final shapes [4]. These simple models of heteropolymers are of additional interest as examples of disordered systems with connections to spin glasses [5], with the advantage of faster relaxation [6,7].

There are a number of recent experimental studies of solutions [8] and gels [6,7] of polymers that incorporate randomly charged groups. As statistical approaches only provide general descriptions of such heteropolymers, we focus on simple models which include the essential ingredients. The overall size and shape of a polymer with charged groups is most likely controlled by the Coulomb interactions that are the strongest and with the longest range. We shall consider the typical properties of a model *polyampholyte* (PA) [9]: a flexible chain in which each of the N monomers has a fixed charge $\pm q_0$ selected from a well defined ensemble of quenches. The polymer has a characteristic microscopic length a (such as the range of the excluded-volume interaction, or nearest neighbor distance along the chain). In the numerical studies we further simplify the model by considering only self-avoiding walk (SAW) configurations on a cubic lattice with lattice constant a.

The long-range nature of the Coulomb interactions, combined with the randomness of the charge sequence, produces effects that are quite distinct from systems with short-range interactions. In Sec. II we use the knowledge accumulated in previous studies [10–15] to explore the phase diagrams of quenched PAs in d dimensions. In particular, we show that for $d > 4$, the behavior of the PAs is similar to that of random chains with short-range interactions, while for $d < 4$ the spatial conformations of a PA strongly depend on its excess charge $Q \equiv \sum_{i=1}^{N} q_i$. In every space dimension $d < 4$, there is a critical charge Q_R such that PAs with $Q > Q_R$ cannot form a compact state. The probability of a randomly charged PA to have such an excess charge depends on both d and its length. In the $N \to \infty$ limit the excess charge will always (i.e., with probability 1) be "small" for $d > 3$ and "big" for $d < 3$. Thus, investigation of the "borderline" three-dimensional case provides valuable insight into the behavior of the system in general space dimensions.

In Sec. III we summarize previous results for PAs in $d = 3$: analytical arguments and Monte Carlo (MC) studies indicate that the PA undergoes a transition from a dense ("globular") to a strongly stretched configuration as Q exceeds $Q_c \approx q_0 N^{1/2}$. The MC simulations [12–15] were performed for polymer sizes up to $N = 128$ and in a wide range of temperatures. They, however, could

not provide information on the energy spectrum of PAs, and on very low temperature properties. In this work we undertake a complete enumeration study of PAs for all possible quenches up to $N = 13$, and are thus able to present very detailed results regarding energetics and spatial conformations of short PAs. The details of the enumeration procedure are explained in Sec. IV, while the results are described in Secs. V and VI. The majority of these results add further support to the predictions of MC studies, and provide some details which could not be measured by MC studies (e.g., density of states, condensation energy, and surface tension in the globular phase). We also find some indication that PAs with small Q may undergo a phase transition between two dense states. No signs of this transition could be detected in the MC studies, because it occurs at temperatures too low for that procedure to equilibrate.

II. POLYAMPHOLYTE PHENOMENOLOGY

It is helpful to view the problem in the more general context of a variable space dimension d. Let us consider a continuum limit in which configurations of the PA are described by a function $\vec{r}(x)$. The continuous index x is used to label the monomers along the chain, while $\vec{r}$ is the position of the monomer in d-dimensional embedding space. The corresponding probabilities of these configurations are governed by the Boltzmann weights of an effective Hamiltonian,

$$\frac{\mathcal{H}[q(x)]}{T} = \frac{K}{2}\int dx \left(\frac{d\vec{r}}{dx}\right)^2 + \frac{v}{2}\int dx\, dx' \delta^d[\vec{r}(x) - \vec{r}(x')] + \frac{1}{2T}\int dx dx' \frac{q(x)q(x')}{|\vec{r}(x) - \vec{r}(x')|^{d-2}} \equiv H_0 + H_v + H_q \ . \quad (1)$$

In this equation, H_0 represents the entropic properties of the connected chain (ideal polymer), H_v is the continuum description of the excluded volume interactions, while H_q represents the d-dimensional electrostatic energy. For each PA, there is a specific (quenched) function $q(x)$ representing the charges along the chain. (In this work we set $k_B = 1$ and measure T in energy units.)

In the simplest ensemble of quenches, each monomer takes a charge $\pm q_0$ independent of all the others; i.e., $\overline{q_i q_j} = \delta_{ij} q_0^2$, where the overline indicates averaging over quenches. While the average charge of such PAs is zero, a "typical" sequence has an excess charge of about $\pm Q_c$, with $Q_c \equiv q_0 N^{1/2}$. This statement, as well as the definition of Q_c, are unrelated to the embedding dimension d. However, the importance of charge fluctuations (both for the overall polymer, or large segments of it) does depend on the space dimension. The electrostatic energy of the excess charge, spread over the characteristic size of an ideal polymer ($R \propto N^{1/2}$), grows as $Q^2/R^{d-2} \sim N^{(4-d)/2}$. This simple dimensional argument shows that for $d > 4$ weak electrostatic interactions are irrelevant. (The excluded volume effects are also irrelevant in $d > 4$.) Thus, at high temperatures the PA behaves as an ideal polymer with an entropy-dominated free energy of the order of $-NT$. However, upon lowering the temperature it collapses into a dense state, taking advantage of a condensation energy of the order of $-Nq_0^2/a^{d-2}$. This collapse is similar to the well known θ transition of polymers with short-range interactions and will be discussed later in this section.

For $d < 4$, electrostatic interactions are relevant and the high temperature phase is no longer a regular self-avoiding walk. At high temperatures the behavior of the polymer can be studied perturbatively. For the above ensemble of uncorrelated charges, the lowest order $(1/T)$ correction to the quench-averaged R_g^2 vanishes [12,13]. However, if we restrict the ensemble of quenches to sequences with a fixed overall excess charge of Q, there is a lowest order correction term proportional to $Q - Q_c$. Thus PAs with Q less than Q_c contract while those with larger charges expand. This trend appears in any space dimension d, and is indicated by the vertical line at the top of Fig. 1. It should be noted that restricting the ensemble to yield fixed Q slightly modifies the quench-averaged charge-charge correlations. In particular, the two-point correlation function becomes $\overline{q_i q_j} = (Q^2 - Q_c^2)/N^2$ for $i \neq j$. This small (order of $1/N$) correction to the correlation function may cause a significant change in R_g^2 due to the long-range nature of the Coulomb interaction.

The above discussion can be extended to PAs with short-range correlations along the sequence: If neighboring charges satisfy $\overline{q_i q_{i+1}} = q_0^2\lambda$ [16] where $-1 < \lambda < 1$, with no further restrictions, then $\overline{q_i q_j} = q_0^2 \lambda^{|j-i|}$. The resulting ensembles continuously interpolate between the deterministic extremes of an alternating sequence ($\lambda = -1$) and a uniformly charged polyelectrolyte ($\lambda = 1$). As in the case of uncorrelated charges, we can impose an additional constraint on the overall charge, resulting in the correlations

$$\overline{q_i q_j} = q_0^2 \lambda^{|j-i|} + [Q^2 - Q_c^2(\lambda)]/N^2 \ , \quad (2)$$

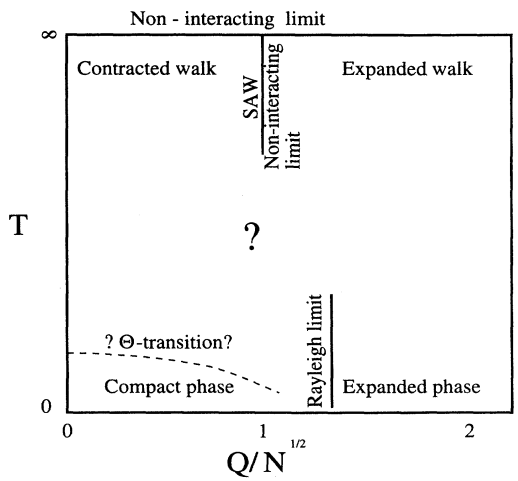

FIG. 1. Qualitative phase diagram of a PA as a function of temperature T and its excess charge Q. See the text for details.

where $Q_c^2(\lambda) = q_0^2 N(1+\lambda)/(1-\lambda)$. We note that the variance of Q in such a correlated sequence also becomes $q_0^2 N(1+\lambda)/(1-\lambda)$. Thus the proportion of quenches with Q above or below $Q_c(\lambda)$ is independent of λ. All the results for uncorrelated sequences remain valid if we substitute $Q_c(\lambda)$ for Q_c. As $|\lambda| \to 1$, the behavior of the PA crosses over from that of a random sequence to the deterministic (alternating or homogeneous) one. However, the crossover occurs only for $|\lambda| - 1 \approx O(1/N)$. As typical of the qualitative behavior outside this narrow interval, we concentrate on the uncorrelated case of $\lambda = 0$.

A short distance cutoff a, such as the range of the excluded volume interaction, introduces a temperature scale q_0^2/a^{d-2}. For $d > 4$ the electrostatic interactions in random PAs are effectively short ranged. Previous results on a random short-range interaction model [17] (RSRIM) in $d = 3$ indicate that, as long as the positive and negative charges are approximately balanced, the polymer assumes spatial conformations where the interactions are predominantly attractive. To maximize this attraction, the chain undergoes a transition from an expanded to a collapsed (dense) state at a θ transition. For truly short-range interactions, the θ transition disappears only for a rather strong charge imbalance of $Q \sim N$. Even if as a result of the relevant Coulomb interactions in $d < 4$, the high temperature phase of uncorrelated PAs turns out to be compact, we cannot exclude the possibility of a transition into another dense (possibly glassy) state when T decreases below a critical θ_E. Such a potential "θ_E transition," as indicated by the horizontal dashed line in Fig. 1, must be different from a regular collapse since the lower density phase is not a self-avoiding walk. The compact phase can also be destroyed by increasing the net charge as described in the following paragraph.

A dense globular PA droplet of radius $R \sim aN^{1/d}$ has a surface energy of γR^{d-1}, where $\gamma \approx q_0^2/a^{2d-3}$ is the surface tension. For small Q, the surface tension keeps the PA in an approximately spherical shape. However, as shown in the Appendix, at sufficiently large Q electrostatic forces destabilize the droplet. Comparing the electrostatic ($\propto Q^2/R^{d-2}$) and surface energies indicates that the droplet shape is controlled by the parameter $\alpha = Q^2/Q_R^2$, where $Q_R \approx q_0 N^{1-3/2d}$ is the *Rayleigh charge*. For a large enough α a spherical shape is unstable (a charged liquid droplet disintegrates). The Rayleigh charge in $d = 3$ is proportional to $Q_c = q_0\sqrt{N}$, while for $d > 3$ ($d < 3$) it increases faster (slower) than Q_c. The solid vertical line at the bottom of Fig. 1 shows the position of this instability in $d = 3$. Clearly, any θ_E transition (if at all present) must also terminate at Q_R. Only a negligible fraction of random quenches in $d > 3$ have Q exceeding Q_R, and thus a typical PA is a spherical droplet at low T. Conversely, in $d < 3$ almost all PAs have charges larger than Q_R and the dense phase does not exist. The borderline case of $d = 3$, where a finite fraction of PAs have Q exceeding Q_R, is the most controversial: An analogy with uniformly charged polyelectrolytes [18] suggests [10] that the PA is fully stretched ($\nu = 1$) in this case [10]. In contrast, a Debye-Hückel inspired theory [11] predicts that low-T configurations are compact. Partial resolution of this contradiction comes from the observation [12,13] that PAs in $d = 3$ are extremely sensitive to the excess charge Q. In the following section we shall briefly review the main features of three-dimensional PAs obtained by MC simulations [14,15].

III. MONTE CARLO RESULTS IN THREE DIMENSIONS

Numerical simulations are performed on a discretized version of Eq. (1). Configurations of a polymer are specified by listing the position vectors $\{\mathbf{r}_i\}$ $(i = 1, \ldots, N)$ of its monomers. The shape and spatial extent of the polymer are then characterized by the tensor,

$$\mathcal{S}_{\mu\nu} = \frac{1}{N}\sum_{i=1}^{N} r_{i\mu} r_{i\nu} - \frac{1}{N^2}\sum_{i=1}^{N} r_{i\mu} \sum_{j=1}^{N} r_{j\nu} , \qquad (3)$$

with the greek indices labeling the various components. Thermal averages of the eigenvalues $\lambda_1 > \lambda_2 > \lambda_3$ of this tensor (sometimes referred to as moments of inertia) are used to describe the mean size and shape; their sum is the squared radius of gyration, $R_g^2 = \mathrm{tr}\mathcal{S}$. Since we are dealing with sequences of quenched disorder, these quantities must also be averaged over different realizations of $\{q_i\}$. In three dimensions, uniform uncharged polymers in good solvents are swollen; their R_g scaling as N^ν with $\nu = 0.588$ as in self-avoiding walks. Polymers in poor solvents are "compact," i.e., described by $\nu = 1/3$.

In previous work [14,15] we used Monte Carlo (MC) simulations (along with analytical arguments) to establish the following properties for PAs immersed in a good solvent.

(a) The radius of gyration strongly depends on the total excess charge Q, and is weakly influenced by other details of the random sequence.

(b) A $1/T$ expansion indicates that the size of a PA tends to decrease upon lowering temperature if Q is less than a critical charge $Q_c \equiv q_0 N^{1/2}$, and increases otherwise. This behavior is confirmed by MC simulations.

(c) At low temperatures, neutral polymers ($Q = 0$) are compact in the sense that their spatial extent in any direction grows as $aN^{1/3}$, where a is a microscopic length scale.

(d) The low-T size of the PA exhibits a sharp dependence on its charge: R_g is almost independent of Q for $Q < q_0\sqrt{N}$, and grows rapidly beyond this point. This increase becomes sharper as the temperature is lowered, or as the length of the chain is made longer.

We interpret the low temperature results by an analogy to the behavior of a charged liquid drop. The energy (or rather the quench averaged free energy) of the PA is phenomenologically related to its shape by

$$E = -\epsilon_c N + \gamma S + \frac{bQ^2}{R}. \qquad (4)$$

The first term is a condensation energy proportional to the volume (assumed compact), the second term is proportional to the surface area S (with a surface tension γ),

while the third term represents the long-range part of the electrostatic energy due to an excess charge Q (b is a dimensionless constant of order unity). The optimal shape is obtained by minimizing the overall energy. The first term is the same for all compact shapes, while the competition between the surface and electrostatic energies is controlled by the dimensionless parameter

$$\alpha \equiv \frac{Q^2}{16\pi R^3 \gamma} = \frac{Q^2}{12 V \gamma} \equiv \frac{Q^2}{Q_R^2} . \tag{5}$$

Here R and V are the radius and volume of a spherical drop of N particles, and we have defined the *Rayleigh charge* Q_R [see Eq. (A3) of the Appendix for the definition of Q_R in a general dimension d]. The dimensionless parameter α controls the shape of a charged drop: A spherical drop becomes unstable and splits into two equal droplets for $\alpha > 0.3$. We argued in Refs. [14,15] that the quenched PA has a similar instability at the vertical line in the bottom of Fig. 1: Charged beyond a critical α, the PA splits to form a *necklace* of blobs connected by strands. From the definition of Q_R it is clear that it is proportional to Q_c; the dimensionless prefactor relating the two depends on γ and is estimated in this work.

(e) While confirming the general features of Fig. 1, the MC simulations provide no indication of the suggested θ_E transition. However, these simulations are not reliable at very low temperatures [19] due to the slowing down of the equilibration process.

All the above results were obtained by MC simulations for PAs of between 16 and 128 monomers. Since the MC procedure does not provide good equilibration at low T, we could not determine the properties of the ground states (although some conclusions were drawn from the low-T data). Systems with Coulomb interactions are particularly poorly equilibrated, even at densities of only 10% the maximal value. To remedy these difficulties, in this work we resorted to a complete enumeration of all possible spatial conformations and all possible quenched charge sequences. While such an approach enables us to obtain exact results, and detailed information not available in MC studies, the immensity of configuration space restricts the calculation to chains of at most 12 steps (13 monomers).

IV. THE ENUMERATION PROCEDURE

We considered self-avoiding walks (SAWs) on a simple cubic lattice of spacing a. An L-step SAW has $N = L+1$ sites (atoms), and the randomly charged polymer is defined by assigning a fixed sequence of charges ($q_i = \pm q_0$) to its monomers. The charge sequence is considered to be quenched, i.e., it remains unchanged when the spatial conformation of the walk changes. The energy of any particular configuration is given by $U = \sum_{i<j} q_i q_j / |\vec{r}_i - \vec{r}_j|$, where $\vec{r}_i$ is the position of the ith atom on the three-dimensional lattice. Thermal averages of various quantities are calculated by summing over all conformations with the Boltzmann weights of this energy. The resulting average is quench specific. We then obtain quenched averages by summing over all possible realizations of the sequence, possibly with certain restrictions such as on the total excess charge $Q \equiv \sum_i q_i$.

Our calculation consists of three steps: (a) Generating lists of all spatial conformations and quench sequences; (b) using the lists to calculate various thermodynamic quantities for each quenched configuration; and (c) averaging of results over restricted ensembles of quenches, and analyzing the data. Since the calculational procedure is extremely time consuming, we used precalculated lists of all SAWs, and of all possible sequences of charges along the chains. Other programs then used these two lists as input. Since the first list of all L-step SAWs with $3 \le L \le 12$ is extremely large, we tried to reduce it by including only "truly different" configurations and listing their degeneracies. As the actual position of a walk in space is not important, we disregard it and only give the *directions* of the L steps. As the energy of a configuration is independent of its overall orientation, we assume that the first step is taken in the $+x$ direction. The above trivial symmetries are not included in our counting; e.g., we assign a completely straight line the degeneracy of $m = 1$. All SAWs, except for the straight line, have a fourfold degeneracy related to rotation around the direction of the initial step. We shall therefore assume that the first step which is not in the $+x$ direction is taken along the $+y$ axis, and attribute a degeneracy $m = 4$ to all walks which are not straight lines. Every nonplanar walk has an additional degeneracy due to reflection in the x-y plane, leading to a total degeneracy of $m = 8$. Thus the list of all 12-step SAWs consists of the directions of 11 successive steps, along with a degeneracy factor. The total number of 4 162 866 chains consists of one straight line ($m = 1$), 40 616 planar SAWs ($m = 4$), and 4 122 249 nonplanar SAWs ($m = 8$). Accounting for degeneracies reduces the length of the list and the time needed to calculate various quantities by almost a factor of 8. Some chains possess additional symmetries; e.g., by inverting the sequence of steps we may get some other SAW in the list. We did not take advantage of this symmetry because the distribution of quenched charges on the chain is not necessarily symmetric under interchange of its two ends. In any case, we use the end to end exchange symmetry in the listing of all possible quenches.

A second input list contains all possible charge sequences; each "quench" for an L-step walk has $N = L+1$ charges. Since the energy is unchanged by reversing the signs of all charges, we considered only configurations in which the total charge is $Q \ge 0$. This shortens the list by almost a factor of 2. The majority of quenches are not symmetric under order reversal, i.e., the sequence does not coincide with itself when listed backwards. Since we are exploring all spatial configurations, without accounting for the end-reversal symmetry mentioned in the previous paragraph, the list can be reduced by almost another factor of 2 by considering only one of each pair of such quenches (keeping track of the degeneracy). After accounting for both charge and sequence reversal symmetries, the list for $L = 12$ ($N = 13$) has only 2080 entries.

For any sequence, the number of computer operations required to calculate the energy of a single configuration

grows as L^2. The total number of SAWs grows as $z^L L^x$, where $z \approx 4.68$ is the effective coordination number for SAWs on a cubic lattice, and $x \approx 0.2$. The number of "quenches" grows as 2^L. These factors limit the size of chains which can be investigated to $L = 12$ steps. At this L we needed four weeks of CPU time on a Silicon Graphics R4000 workstation. An increase of L by a single unit multiplies the calculation time by an order of magnitude. Thus it is impractical to employ our procedure for chains that are much longer than 12 steps. If, instead of completely enumerating all possible charge configurations we confine ourselves to sampling a few hundred quenches, the calculations can be extended to $L = 13$, but not much further.

The order in which the calculations were performed is as follows: for each SAW configuration we calculated the radius of gyration, squared end-to-end distance, *and* the energies of all possible quenched charge configurations along the backbone. These energies were then used to update histogram tables (a separate histogram of possible energies for each quench). Due to the long-range nature of the Coulomb interaction, the allowed energies form almost a continuous spectrum which we discretized in units of $0.1q_0^2/a$. This discretization was sufficient to accurately reproduce properties of the system on the temperature scales of interest. (For $L < 10$, we used a finer division of the histograms to verify that the discretization process does not distort calculation of such properties as the specific heat, except at extremely low temperatures.) In addition to histograms, we also collected data about the energy, the radius of gyration, and the end-to-end distance at the ground state of each quench.

The issue of the multiplicity of the ground state is of much interest, and hotly debated in the context of models of proteins [20]. In the presence of Coulomb interactions, due to the quasicontinuous nature of the energy spectrum, the ground state is almost never degenerate (except for the trivial degeneracies mentioned above). It is quite likely that, for sufficiently long polymers and specific quenches, there may be exactly degenerate ground states which are not related by symmetry operations. However, for $L \leq 12$ such cases are extremely rare. Moreover, the distance between the ground state and the second-lowest energy state remains of the order of $0.1q_0^2/a$ for all L's in our calculation, even though at higher energies the densities of the states increase very rapidly with L.

We used these data to obtain averages over quenches (with or without a constraint on the net charge). It should be mentioned that creation of histograms, as well as calculation of the thermal averages, required the correct accounting of degeneracies of spatial conformations, while averages over quenches needed proper care of the sequence degeneracies. For few selected quenches we also performed a calculation of the density of states as a function of two variables, the energy and the squared radius of gyration. Due to large amount of data, we could not do such detailed studies for all possible quenches.

Figure 2 depicts ground states of four cases of quenched charges with different excess charges Q. It provides qualitative support for the conclusions previously obtained from MC simulations: Fig. 2(a) depicts the ground state configuration of an almost neutral PA which is quite compact. The PA in Fig. 2(b) has Q slightly smaller than Q_c; while the configuration is still compact we see the beginning of a stretching. Figures 2(c) and 2(d) show strongly stretched configurations in cases where Q exceeds Q_c. In the following sections we will quantify these qualitative observations.

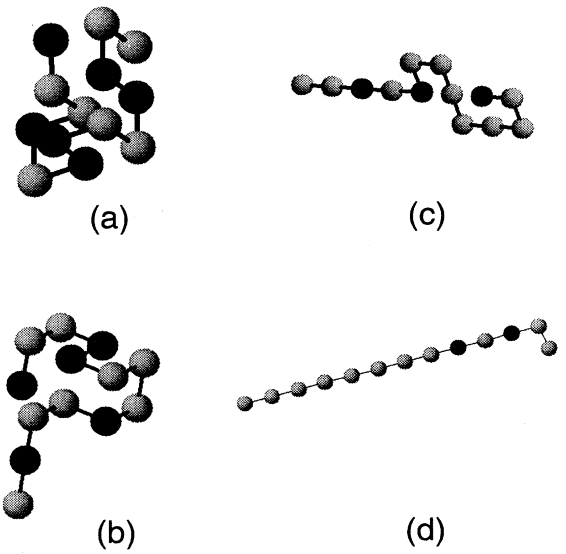

FIG. 2. Spatial conformations of ground states for a sample of $L = 12$ PAs, for values of Q/q_0 equal to (a) 1, (b) 3, (c) 7, and (d) 9. Dark and bright shades indicate opposite charges.

As a by-product of the above procedure we also obtained similar data for the model with short-range interactions: In the random short-range interaction model (RSRIM), a quenched sequence of dimensionless charges $q_i = \pm 1$ is defined along the chain. The interaction energy is $U = \sum_{i<j} V_{ij}$, where $V_{ij} = v_0 q_i q_j$ if $|\vec{r}_i - \vec{r}_j| = a$, and $= 0$, otherwise. While we shall compare and contrast several properties of short- and long-range models in this paper, detailed results for RSRIM can be found in Ref. [17]. The additional data were gathered without a substantial increase in the total execution time of the programs. There are a few minor differences in the data collection process in the two models: (a) As the energies of the RSRIM are naturally discretized, the resulting histograms are exact. (b) The ground state of most quenches is highly degenerate. This required keeping track of the degeneracy, and obtaining the R_g^2 in the ground state as an average lowest energy configurations.

V. ENERGY SPECTRA OF QUENCHED POLYAMPHOLYTES

We begin our analysis by testing the validity of Eq. (4) for the ground states of the polymers. Obviously, the exact value of each ground state energy depends on the details of the charge sequence. However, Eq. (4) implies that the effect of the overall charge can be (approximately) separated; the remaining parts of the en-

ergy depending only weakly on the details of the sequence. The basic energy unit of our model is q_0^2/a, and a useful system for comparison is the regular crystal formed by alternating charges (the "sodium chloride" structure). The condensation energy per atom of such a crystal ($\epsilon_{c0} = 0.8738 q_0^2/a$) is much smaller than the interaction energy per atom between the nearest neighbors ($3q_0^2/a$). This demonstrates the importance of the long-range Coulomb interaction: although the system is locally neutral, the ground state energy depends on an extended neighborhood. Similarly, the surface tension $\gamma_0 = 0.03 q_0^2/a^3$ of the crystal is quite small.

Our first observation is that, for a fixed Q, the ground state energy is quite insensitive to the details of the sequence: Figure 3 depicts the ground state energies of *all* 2080 possible quenches for 12-step (13-atom) chains. (The horizontal axis represents an arbitrary numbering of the quenches.) The energies are clearly separated into seven bands, corresponding to excess charges of $Q = 1$, 3, 5, ..., 13. (There is only one quench with $Q = 13$.) While each band has a finite width, we see that the energy of a PA can be determined rather accurately by only specifying its net charge Q. This is *not* the case for *short-range* interactions: A comparison of histograms of ground state energies between (a) PAs and (b) the RSRIM of length $L = 10$ in Fig. 4 clearly shows the importance of long-range interactions. There is a rather clear separation of energies into "bands" with fixed values of Q for the PAs, which is almost absent in the RSRIM. Of course, the finite width of each band shows that the details of the sequence cannot be completely neglected, although their influence on the ground state energy is rather small.

Using a Debye-Hückel approximation [21], Wittmer *et al.* [16] have performed a systematic study of the dependence of the free energy of neutral PAs ($Q = 0$) at high T on the correlations between neighboring charges along the chain [see Eq. (2)]. They obtain an expression which smoothly interpolates between the free energy densities of a completely random sequence ($= -T\kappa^3/12\pi$, where κ^{-1} is the Debye screening length), and a nonrandom alternating sequence ($= -0.0015 T\kappa^4 a$) (the latter model was also studied in Ref. [22]). These results exclude the electrostatic self-interaction energy, which is infinite in the continuum model used in Ref. [16]. Thus the free energy of the alternating chain is roughly 20 times smaller

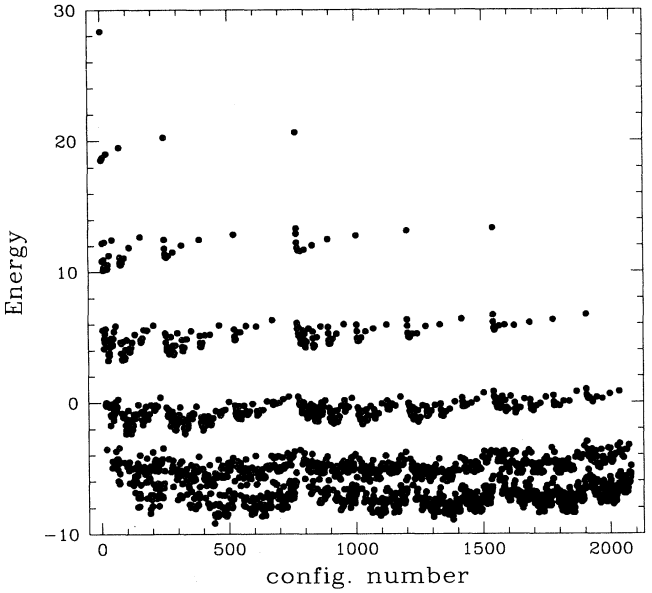

FIG. 3. Energies of the ground states [23] of all distinct (i.e., unrelated by symmetry transformations) quenches (arbitrarily numbered from 1 to 2080) of PAs with $L = 12$.

than the random one. While these results cannot be directly extended to the ground states, we may attempt to obtain crude estimates by setting $\kappa^{-1} = a$ and $T = q_0^2/a$. However, our results indicate that the ground state energy of alternating polymers ($= \epsilon_{c0}$) is only smaller by about 16% than the mean condensation energy of unrestricted sequences. Such an inconsistency is partially explained by the fact that the alternating PA has negative mean electrostatic energy (approximately $0.6 q_0^2/a$ per atom) even at $T = \infty$, while such an energy for a completely random PA (averaged over all quenches) vanishes. Thus, only about 1/4 of the ground state energy of an alternating PA is its condensation energy. (This part of the energy explicitly depends on the discreteness of the chain and is not accounted for in Ref. [16].) This argument brings the approximate conclusions based on Ref. [16] in better qualitative agreement with our exact enumeration results.

The dependence of the quench-averaged ground state

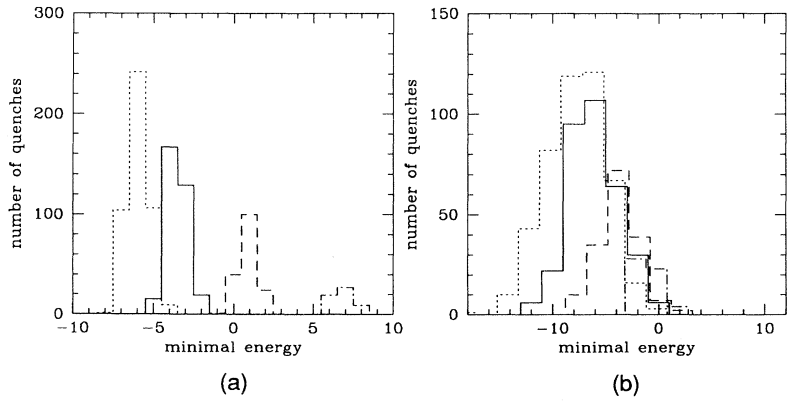

FIG. 4. Histograms of the numbers of ground states versus their energies [23] for chains of length $L = 10$ with charges $Q = 1$ (dotted line), $Q = 3$ (solid line), $Q = 5$ (dashed line), and $Q = 7$ (dot-dashed line) for (a) PAs and (b) polymers with random short-range interactions. The size of the energy bins for these histograms is $\Delta E = 1$.

energies on the length of the chain is depicted in Fig. 5. A restricted average is performed at each value of Q (indicated next to each line). The scaling of the axes is motivated by the recasting of Eq. (4) in the form

$$\frac{E}{N} - \frac{A}{N^{1/3}} = -\epsilon_c + \frac{bQ^2}{aN^{4/3}} , \qquad (6)$$

where $A \equiv \gamma S/N^{2/3} = p\gamma a^2$, with a prefactor p depending on the average shape. The small number of data points makes an accurate determination of A (and hence the surface tension) rather difficult. Of course, the application of Eqs. (4) and (6) to such short chains is problematic. The value used in Fig. 5 is $A = 0.6q_0^2/a$, for which the curves with different Q extrapolate to approximately the same value, giving a condensation energy of $\epsilon_c = (0.75 \pm 0.01)q_0^2/a$. For this choice of A the slopes of the curves with $Q = 1, 2, 3$ approximately scale as Q^2. The condensation energy ϵ_c is surprisingly close to that of a regular crystal ($\epsilon_{c0} = 0.8738q_0^2/a$), despite the fact that in a random chain on average one neighbor (along the chain) has the "wrong" sign (compared to the alternating arrangement), costing an energy of the order of ϵ_{c0}. This again confirms our contention that the ground state energy is determined by very extended neighborhoods of each particle. If the ground state configuration has approximately cubic or spherical shape, then $p \approx 5$, while for the slightly elongated objects that we obtain, p can be somewhat larger ($\approx$8). Therefore, we estimate $\gamma = (0.09 \pm 0.03)q_0^2/a$. The error bars indicate our uncertainty in the values of p and A, and disregard possible systematic errors in attempts to evaluate surface tension from such small clusters. Using these numbers we estimate that the Rayleigh charge of the model PA is approximately the same as Q_c, since

$$Q_R^2 = 12\gamma V \approx 12\frac{0.09q_0^2}{a}aN^3 \approx q_0^2 N = Q_c^2 . \qquad (7)$$

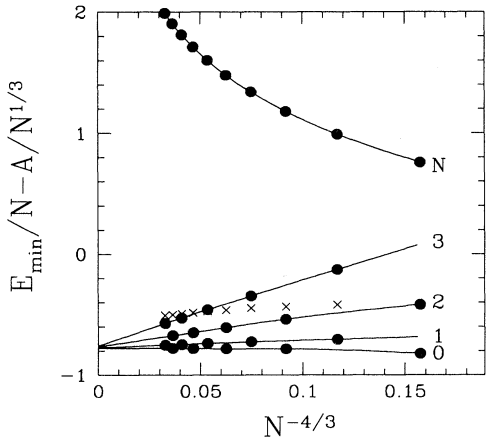

FIG. 5. Ground state energy (per particle) [23] as a function of the number of particles. Each full circle represents a quench average at the values of Q denoted by the numbers near the solid lines. ($Q = N$ corresponds to a fully charged polyelectrolyte.) The $\times$ symbols denote the average over all quenches, unrestricted in charge.

(The relation $V = a^3N$ assumes PAs of maximum possible density.) From Fig. 5 it is not clear that the (charge unconstrained) average energies (indicated by the $\times$ symbols) of all quenches also extrapolate to the same condensation energy of ϵ_c. This apparent inconsistency can be understood by noting that since the quench averaged Q^2 is equal to $q_0^2 N$, the last term in Eq. (6) scales as $N^{-1/3} = (N^{-4/3})^{1/4}$. Thus, the linear approach (in the variables used in Fig. 5) to asymptotic value (as $1/N^{4/3} \to 0$) is replaced by a very small power law. Such a slow decay cannot be detected from the small values of N used in our enumeration study.

Since our model is defined on a discrete lattice, the allowed energies are discrete. However, as the length of the chain increases the separations between the states are reduced. The density of states becomes quasicontinuous and can be described by a function $n(E)$. Figure 6 depicts $s(E) \equiv \ln\overline{n(E)}/N$, where the overline denotes averaging over all quenches with a fixed Q. (Note that this quantity is *not* the quench-averaged free energy as the average is performed on n rather than on $\ln n$.) Not surprisingly, the densities of states for different Q's are shifted with respect to each other. For every quench the density of states is very high near the middle of the band and decreases towards the edges.

We find that almost all PAs have a unique ground state (up to trivial symmetry transformations). This is not the case for short-range interactions [20] and may be an important clue to the problem of protein folding. (For ease of calculation, most studies of similar random copolymers have focused on short-range interactions, and typically find highly degenerate ground states.) Furthermore, the gaps to the second lowest energy states typically remain of order of $0.1q_0^2/a$ (up to the studied size of $L = 12$), while most interstate separations decrease with L. In the $L \to \infty$ limit, the density of lowest energy excitations of our model PAs appears to decay faster than a power law. (Of course our lattice model does not include any vibrational modes.) This decay manifests itself in a vanishing heat capacity in the $T \to 0$ limit, as depicted in Fig. 7.

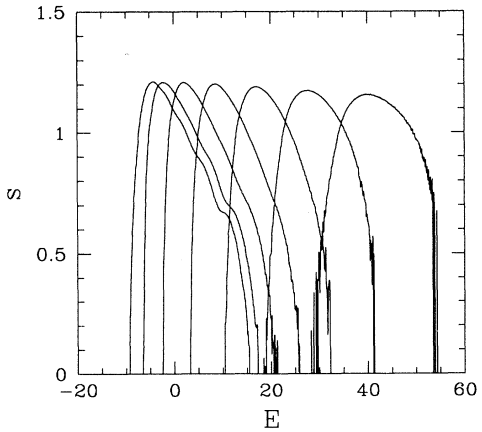

FIG. 6. Logarithms of quench-averaged densities of states per atom (see text) for chains of $L = 13$ with the excess charge Q set to 1, 3, 5, ..., 13 (from left to right).

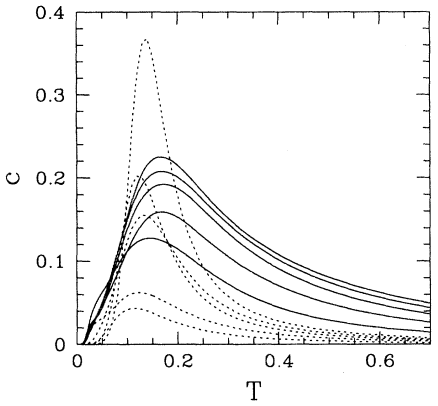

FIG. 7. The quench-averaged heat capacity per degree of freedom for a random PA with $Q = 0$ (solid lines) and $L = 3$, 5, 7, 11 (from bottom to top); and for alternating-charge sequences (dashed lines) of similar lengths.

The solid lines represent the quench-averaged heat capacities per degree of freedom c, of PAs with $Q = 0$ at low temperatures. (Since the energy fluctuations of a polymer depend only on changes of its shape, and are independent of its overall position and orientation, we assumed that an N-atom PA has $3N - 5$ degrees of freedom, where -5 represents a subtraction of translational and rotational degrees of freedom. Such a choice decreases the bias in the N dependence of c which would appear for very small values of N.) The vanishing heat capacity was *not* observed in MC studies [14,15], where poor equilibration at low T hinders measurement of c.

It is instructive to compare and contrast the behavior of random PAs with vanishing excess charge to that of an ordered alternating sequence; the latter is a highly atypical member of the ensemble with $Q = 0$. Numerical investigations of alternating charge sequences by Victor and Imbert [22] show that such polymers undergo a collapse transition, similar to SAWs with *short-range* attractive interactions. This is because the exact compensation in the charges of any pair of neighboring monomers leads to large scale properties determined by dipole-dipole (and faster decaying) interactions. Thus Coulomb interactions are irrelevant in the high temperature phase of the alternating chain that consequently behaves as a SAW. By contrast, even though we consider a subensemble of quenches with $Q = 0$, the charge fluctuations cannot be neglected in random PAs and control the long distance behavior of the chain. Such PAs are compact at *any* temperature.

The attractive dipole-dipole interactions eventually cause the collapse of the alternating charge sequence to a compact state at temperatures below a θ point. Of course, the ground state of such a chain is the ordered NaCl crystal discussed earlier. However, it is not clear if the state of the chain immediately below the θ temperature is the ordered crystal. Another possibility is that the initial collapse is into a "molten globular" (liquid like) state [3], which then crystallizes at a lower temperature. We singled out the alternating PAs in our complete ensemble of quenches; the dashed lines in Fig. 7 depict the heat capacity of this sequence. The presence of a phase transition manifests itself in the peak in c at $T \approx 0.14q_0^2/a$ (for $L = 11$) which grows (and slightly shifts towards higher temperatures) as L increases. Figure 7 shows that the average heat capacity of random PAs with $Q = 0$ also has a peak at $T \approx 0.17q_0^2/a$ (for $L = 11$). As the high temperature phase is no longer swollen (for $Q = 0$), there are again two possible interpretations of this heat capacity peak. One is that it represents a crossover remnant of the θ transition, with an increase in the density of the compact polymer. Indeed, the peak is lower and broader than that of alternating chains. Another possibility is that there is a "glass" transition in which the "molten globule" freezes into its "ground state." The proximity of the peak temperature to the energy gap for the first excited state supports the latter conclusion.

No corresponding anomaly was observed in the MC simulations [14,15]. Since finite size effects are extremely important in such small systems, the heat capacity peak should be regarded only as a suggestion for the presence of a "θ_E transition." As indicated by the dashed line in Fig. 1, the location of such a transition may depend on Q, disappearing at $Q \approx q_0\sqrt{N}$, consistent with other features of the phase diagram. This behavior is analogous to that of the θ point in the RSRIM [17], although in that case the limiting charge scales linearly with N. Additional studies are needed to establish the θ_E transition.

VI. POLYMER SHAPES

The contour plots in Fig. 8 depict the number of states as a function of both R_g^2 and E for three sequences of $L = 10$ with charges $Q = 1$ (a), 5 (b), and 11 (c). At high temperatures the typical configurations correspond to the highest densities. In all three cases these configurations are located in the middle of the diagram and behave essentially as SAWs. On lowering the temperature the polymer seeks out states of lowest energy which are very different in the three cases. The approximately neutral chain of Fig. 8(a) assumes a very compact shape represented by the lower-left corner of the contours. The presence of a specific heat peak is consistent with the shape of this contour plot. While R_g^2 increases monotonically with T, the chains are too short to permit a quantitative test for the presence of a θ_E point from the scaling of R_g^2. The lowest energy contour of the chain with $Q = 5$ [Fig. 8(b)] is almost horizontal. Hence, upon lowering the temperature the chain will not collapse, maintaining an extended shape. Thus a putative transition must disappear for larger Q. Finally, the fully charged polymer in Fig. 8(c) expands from a SAW to the completely stretched configurations represented by the lower-right corner of the contour plot.

The low temperature results from MC simulations suggest that R_g^2 of a PA strongly depends on its charge, crossing over from compact configurations at small Q to extended states for larger Q. This is qualitatively supported by the ground state shapes in Fig. 2, and will be more quantitatively examined here. Figure 9(a) depicts

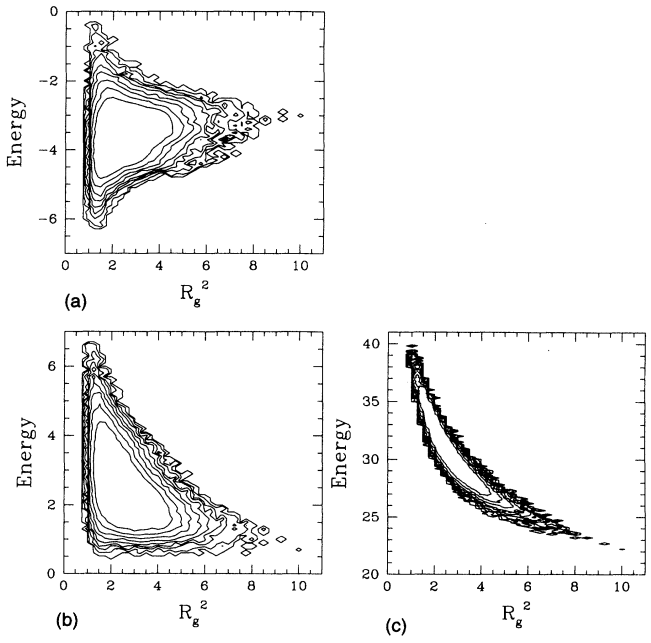

FIG. 8. Contour plots of the number of levels as a function of R_g^2 (in lattice constants) and E (in units of q_0^2/a). The size of each bin is 0.1 in the E direction, and 0.25 in the R_g^2 direction. The contours represent continuous interpolations at levels 0.5, 33, 129, 513, 2049, and 8193. Each plot represents a single chain with $L = 10$ and excess charge Q of (a) 1, (b) 5, and (c) 11.

the L dependence of R_g^2 for several choices of Q. The vertical axis is scaled so that compact, i.e., fixed density, structures are represented by horizontal lines. Since Q is fixed, the influence of the excess charge diminishes as the length of the polymer is increased, and thus all curves must asymptotically converge to the same horizontal line. There is some indication of this in Fig. 9(a), although the crossover is rather delayed for larger values of Q. Since the unrestricted ensemble (solid circles) includes a large range of Q's, it is not surprising that the corresponding averages are not compact. The chains are too short to extract a meaningful value for the exponent ν. Nevertheless, the effective slope of $\nu_{\text{eff}} \approx 1/2$ strongly suggests that the average over an unrestricted ensemble is not compact. By comparison, the corresponding results for the RSRIM in Fig. 9(b) clearly indicate that the averages both at fixed and varying Q have similar fixed density ground states.

Since the quench-averaged R_g^2 of the unrestricted ensemble scales differently from the subensembles of fixed Q, the former set must contain a non-negligible portion of noncompact configurations for every L. It is natural to assume that the borderline between compact and stretched states is controlled by $Q_c = q_0\sqrt{N}$. In previous work [14,15] we argued that PAs undergo a transition to an expanded state when Q exceeds Q_R ($\propto Q_c$): the transition is more pronounced for larger L and lower T. In the MC simulations [14,15] we were able to use long PAs, but were restricted to finite, albeit small, temperatures which slightly smeared the transition in R_g with increasing Q. In this study we know the exact ground states but are limited to small Ls where the difference between R_g of compact and stretched states is less visible. The sum of all eigenvalues of the shape tensor, R_g^2 is somewhat insensitive to an expansion since the increase in the largest eigenvalue is partially compensated by the decrease of the other two eigenvalues. A clearer view is provided by the ratios of the mean eigenvalues of the shape tensor as depicted in Fig. 10. These ratios for different L's can be collapsed after scaling the charges by Q_c, consistent with the MC simulations.

Figure 11 depicts (on a logarithmic scale) the distribution of values of R_g^2 in the ground states of all quenches for $L = 13$. The distribution is peaked near the smallest possible value of R_g^2, but has a broad (possibly power law) tail. If the tail falls off sufficiently slowly, it will determine the asymptotic value of the exponent ν: As L increases the very large values of R_g^2 of the (minority) stretched configurations will eventually dominate the total average. We thus expect ν_{eff} to increase with L, and the value of ν_{eff} extracted from the slope of the solid line on Fig. 9(a) probably underestimates the true asymptotic value. To get further insight into the behavior for larger L, we performed separate averages for the 80% of configurations which have the smallest R_g^2, and for the remaining top 20%. These averages are depicted in Fig. 12. The vertical axis is again scaled so that compact structures are represented by horizontal lines. The bottom 80% indeed scale as compact chains while the top 20%, which stand for the tail of the distribution, have radii that grow with L with an effective exponent of $\nu_{\text{eff}} \approx 2/3$. We

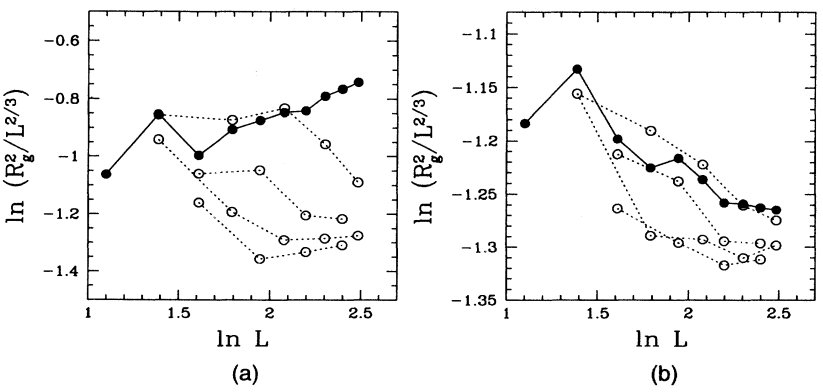

FIG. 9. Quench-averaged scaled R_g^2 as a function of the length of the polymer for (a) PAs with electrostatic interactions, and (b) random polymers with local interactions. Open circles and dashed lines represent (from bottom to top) the restricted averages with $Q = 0, 1, 2, 3$. Full circles and the solid line represent unrestricted averages.

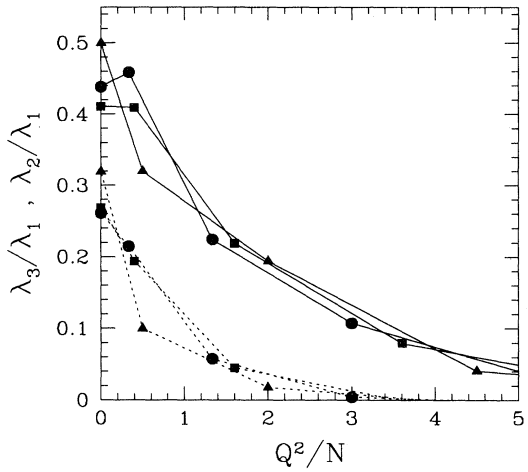

FIG. 10. Ratios between the smallest and largest eigenvalues of the shape tensor (dashed lines), and between the intermediate and largest eigenvalues (solid lines), for $L = 8$, 10, and 12 (full triangles, squares, and circles, respectively) as a function of the scaled charge Q/Q_c. The eigenvalues are calculated from quench averages at fixed Q.

thus conclude that the R_g^2 of the unrestricted ensemble increases with L at least as fast as a SAW.

VII. ANNEALED POLYAMPHOLYTES

As a byproduct of our study, since we have access to the complete set of quenches, we can find which particular sequence, restricted only by its net charge, has the lowest energy. As this is the sequence that is selected in a model in which the charges are free to change positions along the chain, we shall refer to the results as describing the ground states of *annealed PAs*. For long chains, neither the sequence, nor its spatial conformation, need to be unique. However, for the sizes considered here, we

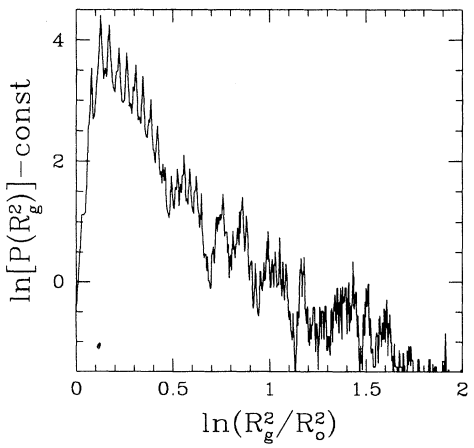

FIG. 11. Probability distribution for R_g^2 of ground states in the unrestricted ensemble of quenches for $L = 12$. R_g^2 is scaled by its minimal possible value, while the scale of the probability is arbitrary.

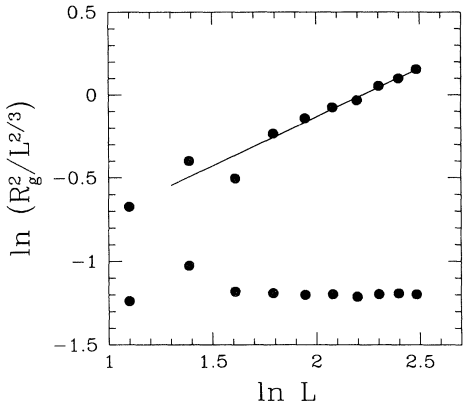

FIG. 12. Scaled partial averages of R_g^2 of the ground states for the 20% of quenches with largest R_gs (top curve), and the remaining quenches (bottom curve) as a function of the length of the PA.

always found a single ground state, several of which are shown in Fig. 13 for $L = 13$ and different values of Q. It appears that the optimal configurations correspond to a uniform distribution of excess charge along the backbone. In particular, for small Q the preferred arrangement is the alternating sequence which then folds into a NaCl structure.

Previously [14,15], we suggested that annealed PAs expel their excess charge (provided $Q > q_0 N^{1/3}$) into highly charged "fingers." As a result of such "charge expulsion" the spanning length of annealed PAs should increase dramatically ($\sim Q$). However, since most of the mass remains in a compact globule, R_g^2 is not substantially modified (as long as $Q < Q_c \sim q_0 N^{1/2}$). The chains used in our study are too short to exhibit an increased spanning length with no change in R_g. Moreover, the

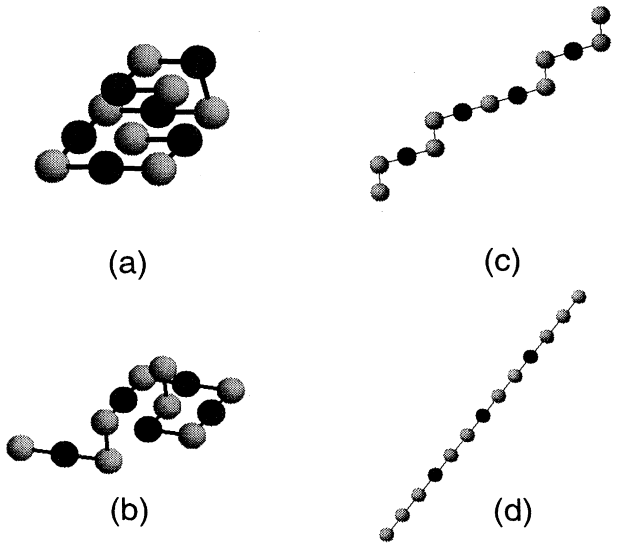

FIG. 13. Spatial conformations of the ground states of annealed PAs with $L = 12$, for values of Q/q_0 equal to (a) 1, (b) 3, (c) 5, and (d) 7. Dark and bright shades indicate opposite charges.

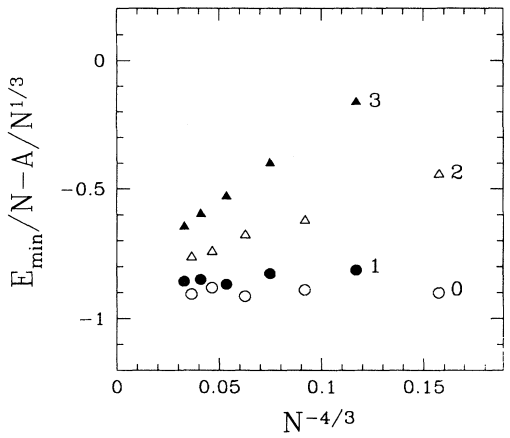

FIG. 14. Ground state energy per atom [23] for annealed PAs as a function of polymer length. Each point represents a single configuration for $Q = 0$, 1, 2, and 3, denoted by open and full circles, and open and full triangles, respectively.

effects of lattice discreteness are much more pronounced for annealed PAs where ground states correspond to a single sequence. In the quenched case, averaging over all sequences partially smooths out lattice effects. As partial evidence we note that plots for the charge dependence of ratios of eigenvalues of the shape tensor (analogous to Fig. 10) exhibit better collapse with the variable $Q/N^{1/3}$ than with $Q/N^{1/2}$. However, given the scatter of the few data points, the evidence for the appearance of "fingers" is not really any more convincing than any conclusions drawn from inspection of the ground states in Fig. 13.

As noted earlier, we expect the ground state of a sufficiently long annealed PA with fixed Q to be the NaCl structure. To test the approach to this limit, in Fig. 14 we plot the energies per atom of the ground states. As in the case of quenched PAs (Fig. 5), we check for finite size corrections proportional to the surface area. (Unlike the case of quenched PAs, each point in this figure represents a *single* configuration.) Here we used a value of $A = 0.35q_0^2/a$ although the results are rather insensitive to this choice, and we estimate the accuracy of this quantity as $\pm 0.10q_0^2/a$. The point of intersection with the $1/N = 0$ axis is close to the known value of the ϵ_{c0}. Furthermore, $A = (0.35 \pm 0.10)q_0^2/a$ corresponds to a surface tension of $0.05 \pm 0.03q_0^2/a^3$ which is also consistent with the known value of γ_0. These consistency checks add further confidence to the values of ϵ_c and γ deduced for quenched PAs.

ACKNOWLEDGMENTS

This work was supported by the U.S.–Israel BSF grant No. 92-00026, by the NSF through Grants Nos. DMR-94-00334 (at MIT's CMSE), DMR 91-15491 (at Harvard), and DMR-93-03667 (M.K.).

APPENDIX: RAYLEIGH INSTABILITY IN ARBITRARY SPACE DIMENSIONS

In this appendix we discuss instabilities of charged d-dimensional drops. A detailed discussion of the three-dimensional case can be found in Appendices B and C of Ref. [15], which also provides other references to the subject. The energy of a charged *conducting* (hyper)sphere of radius R with charge Q is given by

$$E = \gamma S_d R^{d-1} + \frac{Q^2}{2R^{d-2}} , \quad (d > 2) \tag{A1}$$

where the first term is the surface energy (γ is the surface tension, and S_d denotes the d-dimensional solid angle), while the second term is the electrostatic energy. (We have used units such that, in d dimensions, the electrostatic potential at a distance r from a charge q is q/r^{d-2}; and $q \ln r$ in $d = 2$.) For small Q, the sphere is stable with respect to infinitesimal shape perturbations. However, when the electrostatic and surface energies are comparable, the drop becomes unstable. To explore this instability we differentiate Eq. (A1) with respect to R to find the pressure difference between the interior and the exterior of the drop as

$$\Delta p = \frac{(d-1)\gamma}{R} - \frac{(d-2)Q^2}{2S_d R^{2d-2}} . \tag{A2}$$

The pressure difference vanishes when Q equals the *Rayleigh charge* Q_R, where

$$Q_R^2 \equiv \frac{2(d-1)}{d-2} S_d \gamma R^{2d-3} . \tag{A3}$$

For $Q \geq Q_R$ a (hyper)spherical shape is unstable to small perturbations; initially the drop becomes distorted and subsequently it disintegrates. Note that $Q_R^2 \sim R^{2d-3} \sim V^{2-3/d}$, where V is the volume of the drop. When applied to PAs, up to a dimensionless prefactor,

$$Q_R^2 \approx q_0^2 N^{2-3/d} . \tag{A4}$$

We can regard the first term in Eq. (A1) as setting the overall energy scale, while the shape of the drop is determined by the dimensionless ratio

$$\alpha \equiv Q^2/Q_R^2 . \tag{A5}$$

While from the above argument we conclude that the spherical shape is (locally) unstable for $\alpha \geq 1$, even for $\alpha < 1$, the energy of the drop can be lowered by splitting into smaller droplets. In particular, we may split away from the original drop a large number n, of small droplets of radius R/n^x and charge Q/n, and remove them to infinity. It can be directly verified that for $1/(d-1) < x < 1/(d-2)$, the total electrostatic energy, total surface area of the small droplets, as well as their total volume, vanishes in the $n \to \infty$ limit. Thus the energy of any charged conducting drop can be lowered to that of an uncharged drop by expelling a large number of "dust particles" which carry away the entire charge. (Of course this argument neglects the finite size of any particles making up the drop.)

The globular phase of a quenched random PA is better represented by a drop of immobile charges. Therefore, we next consider a drop in which the charges are *uniformly* distributed over the volume. The sum of the surface and

electrostatic energies is now given by

$$E_1 = \gamma S_d R^{d-1} + \frac{d}{d+2}\frac{Q^2}{R^{d-2}} \ . \qquad \text{(A6)}$$

For sufficiently large Q, the drop can lower its energy by splitting into two droplets of equal size. This will occur when α exceeds a critical value of

$$\alpha_d = \frac{2^{1/d}-1}{1-2^{-2/d}}\frac{(d^2-4)}{2d(d-1)} \ , \qquad \text{(A7)}$$

which is equal to 0, 0.293, 0.323, 0.322, and 1/4, for $d = 2$, 3, 4, 5, and ∞, respectively. As the value of α increases further, the drop splits into a larger number of droplets. By examining the energy of a system of n equal spherical droplets, we find that the optimal number is proportional to $\alpha^{d/3}$. If the typical Q^2 is proportional to N (as happens in unrestricted PAs), while Q_R^2 is given by Eq. (A4), the number of droplets scales as $N^{1-d/3}$. Thus $d = 3$ is a special dimension, above which a typical PA prefers to stay in a single globule.

[1] P.G. de Gennes, *Scaling Concepts in Polymer Physics* (Cornell University Press, Ithaca, 1979).

[2] See, e.g., T.E. Creighton, *Proteins: Their Structure and Molecular Properties* (Freeman, San Francisco, 1984).

[3] D.L. Stein, Proc. Natl. Acad. Sci. USA **82**, 3670 (1985); J.D. Bryngelson and P.G. Wolynes, *ibid.* **84**, 7524 (1987); H.S. Chan and K.A. Dill, Physics Today **46**(2), 24 (1993).

[4] T. Garel and H. Orland, Europhys. Lett. **6**, 307 (1988); E.I. Shakhnovich and A.M. Gutin, Europhys. Lett. **8**, 327 (1989); M. Karplus and E.I. Shakhnovich, in *Protein Folding*, edited by T.E. Creighton (Freeman & Co., New York, 1992), Chap. 4, p. 127.

[5] M. Mézard, G. Parisi, and M.A. Virasoro, *Spin Glass Theory and Beyond* (World Scientific, Singapore, 1987).

[6] X.-H. Yu, A. Tanaka, K. Tanaka, and T. Tanaka, J. Chem. Phys. **97**, 7805 (1992); Yu X.-H., Ph.D. thesis, MIT, 1993 (unpublished).

[7] M. Annaka and T. Tanaka, Nature **355**, 430 (1992).

[8] M. Scouri, J.P. Munch, S.F. Candau, S. Neyret, and F. Candau, Macromol. **27**, 69 (1994).

[9] C. Tanford, *Physical Chemistry of Macromolecules* (Wiley, New York, 1961).

[10] Y. Kantor and M. Kardar, Europhys. Lett. **14**, 421 (1991).

[11] P.G. Higgs and J.-F. Joanny, J. Chem. Phys. **94**, 1543 (1991).

[12] Y. Kantor, H. Li, and M. Kardar, Phys. Rev. Lett. **69**, 61 (1992).

[13] Y. Kantor, M. Kardar, and H. Li, Phys. Rev. E **49**, 1383 (1994).

[14] Y. Kantor and M. Kardar, Europhys. Lett. **27**, 643 (1994).

[15] Y. Kantor and M. Kardar, Phys. Rev. E **51**, 1299 (1995).

[16] J. Wittmer, A. Johner, and J.F. Joanny, Europhys. Lett. **24**, 263 (1993).

[17] Y. Kantor and M. Kardar, Europhys. Lett. **28**, 169 (1994).

[18] P. Pfeuty, R.M. Velasco, and P.G. de Gennes, J. Phys. (Paris) Lett. **38**, L5 (1977).

[19] The Coulomb potential used in Refs. [14,15] was slightly distorted at short distances, with different short-range cutoff and intermonomer distances. Therefore, there is no exact equivalence between T of this work and that in Refs. [14,15]. An approximate correspondence is obtained by multiplying the T's in Refs. [14,15] by a factor of 2 to 3.

[20] See, e.g., H. Frauenfelder and P.G. Wolynes, Physics Today **47**(2), 58 (1994).

[21] L.D. Landau and E.M. Lifshitz, *Statistical Physics* (Pergamon, New York, 1981), Pt. 1.

[22] J.M. Victor and J.B. Imbert, Europhys. Lett. **24**, 189 (1993).

[23] In all figures in this paper lengths are measured in units of a, charges in units of q_0, temperatures and energies in units of q_0^2/a. For the RSRIM, charges are dimensionless, and energies are instead measured in units of v_0.